AUSTRALASIAN JOURNAL OF COMBINATORICS
Volume **70(1)** (2018), Pages 104–122

Geometric and combinatorial structure of a class of spherical folding tesselations — II*

Catarina P. Avelino† Altino F. Santos

Centre of Mathematics of the University of Minho — UTAD Pole (CMAT-UTAD)
University of Trás-os-Montes e Alto Douro, Vila Real
Portugal
cavelino@utad.pt afolgado@utad.pt

Abstract

The classification of the dihedral folding tessellations of the sphere whose prototiles are a kite and an equilateral or isosceles triangle was recently achieved. In this paper we complete the classification of spherical folding tessellations by kites and scalene triangles, where the shorter side of the kite is equal to the longest side of the triangle, initiated in [C.P. Avelino and A.F. Santos, *Czech. Math. J.* (to appear)]. The combinatorial structure of each tiling is also analyzed.

1 Introduction

A *folding tessellation* or *folding tiling* (f-tiling, for short) of the sphere S^2 is an edge-to-edge finite polygonal tiling τ of S^2 such that all vertices of τ satisfy the angle-folding relation, i.e., each vertex is of even valency and the sums of alternating angles around each vertex are equal to π.

F-tilings are intrinsically related to the theory of isometric foldings of Riemannian manifolds, introduced by Robertson [8] in 1977. In fact, the edge-complex associated to a spherical f-tiling is the set of singularities of some spherical isometric folding.

The classification of f-tilings was initiated by Breda [6], with a complete classification of all spherical monohedral (triangular) f-tilings. Afterwards, in 2002, Ueno and Agaoka [9] have established the complete classification of all triangular monohedral tilings of the sphere (without any restrictions on angles).

The classification of the dihedral folding tessellations of the sphere whose prototiles are a kite and an equilateral or isosceles triangle was obtained in recent papers, [1, 2, 3, 4]. The study involving scalene triangles is clearly more unwieldy and was

* This research was partially supported by Fundação para a Ciência e a Tecnologia (FCT) through projects UID/MAT/00013/2013 and UID/Multi/04621/2013.

† Also at: Center for Computational and Stochastic Mathematics (CEMAT), University of Lisboa (IST-UL), Portugal.

initiated in [5]. In this paper we complete the classification of dihedral folding tilings of the sphere by kites and scalene triangles in which the shorter side of the kite is equal to the longest side of the triangle.

A spherical kite K (Figure 1(a)) is a spherical quadrangle with two congruent pairs of adjacent sides, but distinct from each other. Let us denote by $(\alpha_1, \alpha_2, \alpha_1, \alpha_3)$, $\alpha_2 > \alpha_3$, the internal angles of K in cyclic order. The length sides are denoted by a and b, with $a < b$. From now on T denotes a spherical scalene triangle with internal angles $\beta > \gamma > \delta$ and side lengths $c > d > e$, see Figure 1(b).

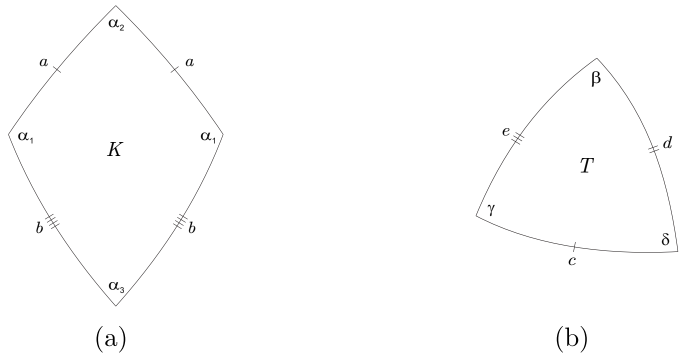

Figure 1: A spherical kite and a spherical scalene triangle

We shall denote by $\Omega(K,T)$ the set, up to isomorphism, of all dihedral folding tilings of S^2 whose prototiles are K and T in which the shorter side of the kite is equal to the longest side of the triangle.

Taking into account the area of the prototiles K and T, we have

$$2\alpha_1 + \alpha_2 + \alpha_3 > 2\pi \quad \text{and} \quad \beta + \gamma + \delta > \pi.$$

As $\alpha_2 > \alpha_3$ we also have

$$\alpha_1 + \alpha_2 > \pi.$$

After certain initial assumptions are made, it is usually possible to deduce sequentially the nature and orientation of most of the other tiles. Eventually, either a complete tiling or an impossible configuration proving that the hypothetical tiling fails to exist is reached. In the diagrams that follow, the order in which these deductions can be made is indicated by the numbering of the tiles. For $j \geq 2$, the location of tiling j can be deduced directly from the configurations of tiles $(1, 2, \ldots, j-1)$ and from the hypothesis that the configuration is part of a complete tiling, except where otherwise indicated.

We begin by pointing out that any element of $\Omega\,(K,T)$ has at least two cells congruent to K and T, respectively, such that they are in adjacent positions and in one and only one of the situations illustrated in Figure 2.

Using spherical trigonometric formulas, and as $a = c$, we obtain

$$\frac{\cos\beta + \cos\gamma\cos\delta}{\sin\gamma\sin\delta} = \frac{\cos\frac{\alpha_3}{2} + \cos\alpha_1\,\cos\frac{\alpha_2}{2}}{\sin\alpha_1\,\sin\frac{\alpha_2}{2}}. \tag{1.1}$$

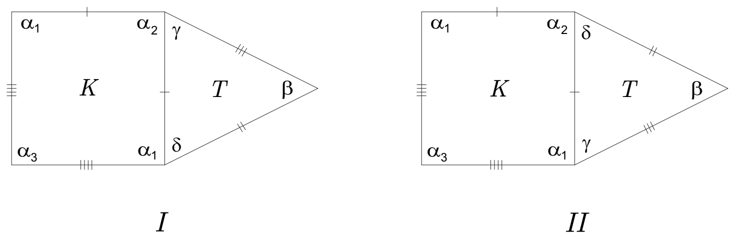

Figure 2: Distinct cases of adjacency

In [5] the case of adjacency I was completely analyzed. In this paper will be addressed the case of adjacency II.

2 Case of Adjacency II

Suppose that any f-tiling with K and T has at least two cells congruent, respectively, to K and T, such that they are in adjacent positions as illustrated in Figure 2-II.

Concerning the internal angles of the kite K, we have necessarily one of the following situations:

$\alpha_1 \geq \alpha_2 > \alpha_3$ or $\alpha_2 > \alpha_1, \alpha_3$ (includes the cases $\alpha_2 > \alpha_1 \geq \alpha_3$ and $\alpha_2 > \alpha_3 > \alpha_1$).

The following propositions address these distinct cases. Throughout we will assume that it is not possible to have angles α_2 and γ glued surrounding a vertex, i.e., two cells congruent to K and T cannot be in adjacent positions as in the first case of adjacency. This follows immediately from the fact that all the f-tilings obtained in [5] do not include vertices surrounded by angles α_2 and δ.

Proposition 2.1. *If $\alpha_1 \geq \alpha_2 > \alpha_3$, then $\Omega(K,T) \neq \varnothing$ if and only if*

(i) $\alpha_1 + \gamma = \pi$, $\alpha_2 + 2\delta = \pi$, $\beta = \frac{\pi}{2}$, $\alpha_1 + \alpha_3 = \pi$ *and* $3\gamma = \pi$, *or*

(ii) $\alpha_1 + \gamma = \pi$, $\alpha_2 + 3\delta = \pi$, $\beta = \frac{\pi}{2}$, $3\gamma = \pi$ *and* $k\alpha_3 = \pi$, *with* $3 \leq k \leq 5$, *or*

(iii) $\alpha_1 + \gamma = \pi$, $\alpha_2 + 2\delta = \pi$, $\beta = \frac{\pi}{2}$ *and* $k\alpha_3 = \pi$, *with* $k \geq 2$.

In the first situation, $\Omega(K,T)$ is composed by a single f-tiling, denote by $\mathcal{M}^3$, where $\delta = \arcsin \frac{\sqrt{3}}{3}$.

In the second situation, for each $k \in \{3,4,5\}$, we obtain a single tiling, denoted by $\mathcal{J}_k$, where $\delta = 2\arcsin \frac{1}{4\cos\frac{\pi}{2k}}$.

In the last case, the angles γ and δ satisfy $\cos\gamma = \cos\frac{\pi}{2k}\sin\delta$ *and, for each $k \geq 2$, $\Omega(K,T)$ is composed by a continuous family of f-tilings, say $\mathcal{S}^k_\gamma$, with $\gamma \in \left(\gamma^k_{\min}, \gamma^k_{\max}\right]$, where*

$$\gamma^k_{\min} = \arccos\left(\cos^2\frac{\pi}{2k}\right) \quad \textit{and} \quad \gamma^k_{\max} = 2\arcsin\frac{\sqrt{8+\cos^2\frac{\pi}{2k}} - \cos\frac{\pi}{2k}}{4}.$$

Remark. In Figures 6(b) and 7 are illustrated the planar and 3D representations of $\mathcal{M}^3$, respectively. A planar representation of $\mathcal{J}_k$ is illustrated in Figure 9. For 3D representations of $\mathcal{J}_k$, $k = 3, 4, 5$, see Figure 10. A planar representation of $\mathcal{S}^k_\gamma$ is illustrated in Figure 11. For 3D representations of $\mathcal{S}^2_\gamma$ and $\mathcal{S}^3_\gamma$ see Figure 13.

Proof. Suppose that any f-tiling with K and T has at least two cells congruent, respectively, to K and T, such that they are in adjacent positions as illustrated in Figure 2-II and $\alpha_1 \geq \alpha_2 > \alpha_3$ $\left(\alpha_1 > \frac{\pi}{2}\right)$.

With the labeling of Figure 3(a), at vertex v_1 we must have $\theta_1 = \gamma$. In fact, if $\theta_1 = \beta$, we have necessarily $\alpha_1 + \beta < \pi$ and $\alpha_1 + \beta + k\alpha_3 = \pi$, for some $k \geq 1$. Nevertheless, we obtain an incompatibility between sides; see Figure 3(b).

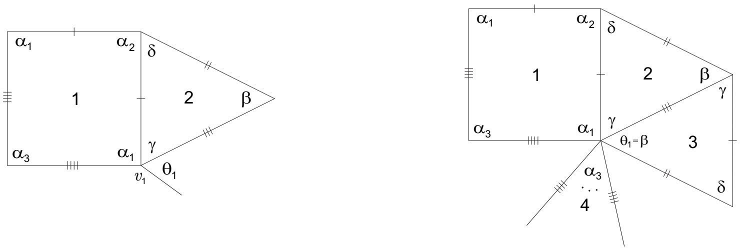

(a) (b)

Figure 3: Local configurations

Now, we have

$$\alpha_1 + \gamma = \pi \quad \text{or} \quad \alpha_1 + \gamma < \pi.$$

1. Suppose firstly that $\alpha_1 + \gamma = \pi$, as illustrated in Figure 4(a). With the labeling of this figure, we have

$$\theta_2 = \beta \qquad \text{or} \qquad \theta_2 = \delta.$$

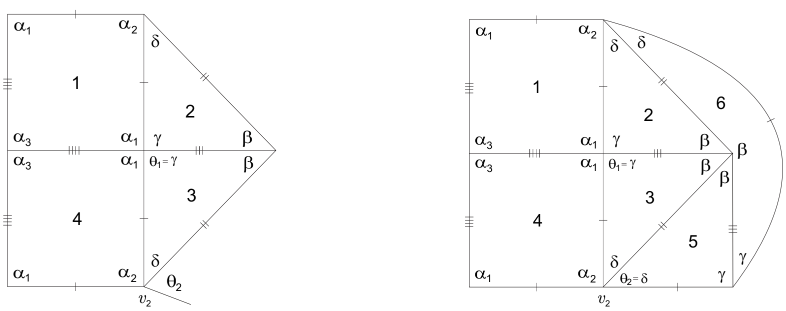

(a) (b)

Figure 4: Local configurations

1.1 If $\theta_2 = \beta$ and *(i)* $\alpha_2 + \beta = \pi$, then we get also $\gamma + \delta = \pi$, which is not possible, as $\alpha_2 > \gamma > \delta$; *(ii)* $\alpha_2 + \beta < \pi$, we have necessarily $\alpha_2 + \beta + k\alpha_3 = \pi$, for some $k \geq 1$, however it is impossible to avoid an incompatibility between sides.

1.2 If $\theta_2 = \delta$, we obtain the configuration illustrated in Figure 4(b). We have $\gamma+\delta > \beta = \frac{\pi}{2}$, $\alpha_1 > \beta$ and $\alpha_1 \geq \alpha_2 > \gamma > \delta$. Note that we must have $\beta + \beta = \pi$, since

- $3\beta > 2\beta + \gamma > \beta + \gamma + \delta > \pi$;
- $2\beta + \alpha_1 > 2\beta + \alpha_2 > \pi$, as $\alpha_1 + \gamma = \pi$ and $(\alpha_1 + \gamma) + (2\beta + \alpha_2) = (\alpha_1 + \alpha_2) + (2\beta + \gamma) > (\alpha_1 + \alpha_2) + (\beta + \gamma + \delta) > 2\pi$;
- it is not possible to have angles α_3 in a vertex surrounded by three angles β due to the dimensions of angles and edges.

Using the fact that two cells congruent to K and T cannot be in adjacent positions as in the first case of adjacency, at vertex v_2 we can have only one of the following possibilities:

(i) $\alpha_2 + \delta + \alpha_2 = \pi$;

(ii) $\alpha_2 + \delta + \alpha_3 \leq \pi$;

(iii) $\alpha_2 + t\delta = \pi$, with $t \geq 2$.

Now, we analyze separately the cases *(i)*-*(iii)*.

(i) If $\alpha_2 + \delta + \alpha_2 = \pi$, we obtain the configuration illustrated in Figure 5(a). As $\alpha_1 + \alpha_1 > \pi$, at vertex v_3 we reach an impossibility.

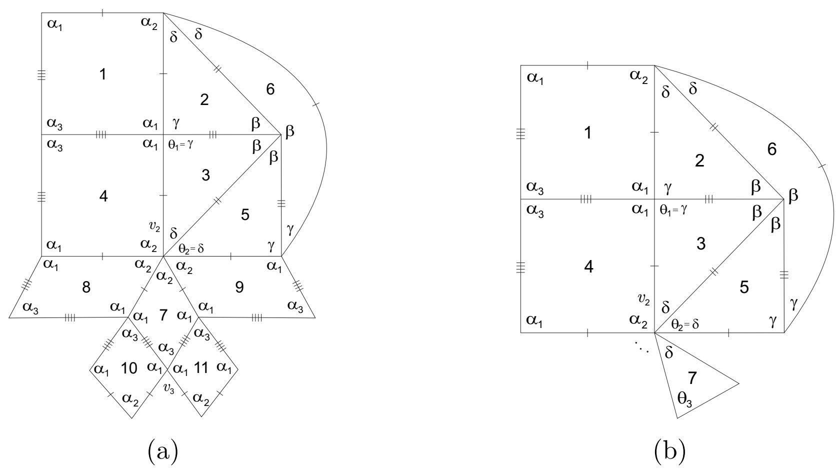

Figure 5: Local configurations

(ii) Similarly, this case also leads to a contradiction, as $\alpha_2 + \delta + \alpha_3 \leq \pi$ implies two angles α_1 on the other alternated sum of v_1.

(iii) Suppose finally that $\alpha_2 + t\delta = \pi$, with $t \geq 2$. With the labeling of Figure 5(b), we have $\theta_3 = \gamma$ or $\theta_3 = \beta$.

(iii)-1. If $\theta_3 = \gamma$, the last configuration extends in a unique way to the one illustrated in Figure 6(a) (note that $\theta_4 = \delta$ implies $\alpha_2 + \delta + \gamma = \pi$ at vertex v_3, which is not

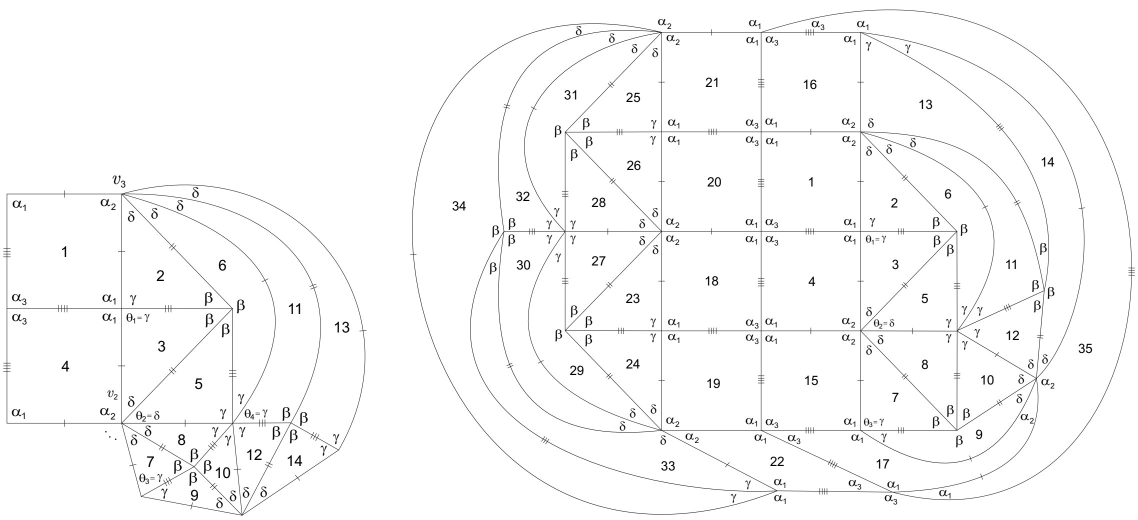

(a) (b) Planar representation of $\mathcal{M}^3$

Figure 6: Local configurations

possible). Observing the vertex of valency six surrounded in cyclic order by tiles (5,6,11,12,10,8) of Figure 6(a), we have $\gamma = \frac{\pi}{3}$. Also, as $\beta + \gamma + \delta > \pi$ and $\beta = \frac{\pi}{2}$, we conclude that $\delta > \frac{\pi}{6}$. By the condition of Case 1.2, $\alpha_2 > \gamma = \frac{\pi}{3}$, and so $\alpha_2 + t\delta = \pi$, $t < 4$. Specifically $t = 2$ or $t = 3$.

If $t = 2$, we have necessarily $\alpha_1 + \alpha_3 = \pi$, otherwise we achieve a vertex with angles α_2 and γ in adjacent positions. Then, the last configuration is extended uniquely to the planar representation illustrated in Figure 6(b). We denote this f-tiling by $\mathcal{M}^3$. We have then $\beta = \frac{\pi}{2}$, $\alpha_1 + \gamma = \alpha_1 + \alpha_3 = \pi$, $\alpha_2 + 2\delta = \pi$, $\gamma = \frac{\pi}{3}$, and so by (1.1), we get $\delta = \arcsin \frac{\sqrt{3}}{3}$. A 3D representation of $\mathcal{M}^3$ is given in Figure 7.

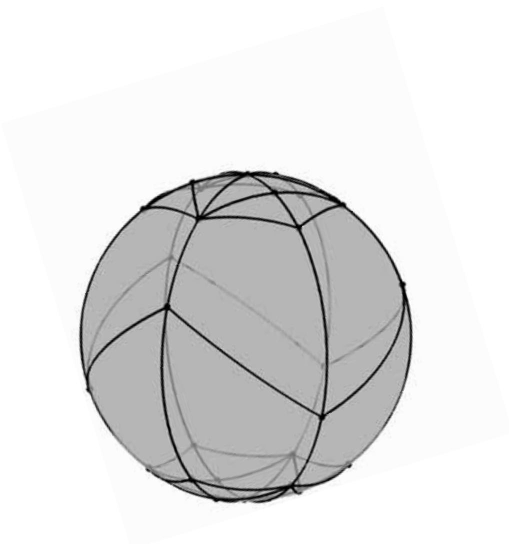

Figure 7: f-tiling $\mathcal{M}^3$

If $t = 3$, we obtain the configuration illustrated in Figure 8(a). If $\theta_4 = \gamma$, it is a straightforward exercise to show that we must have $\alpha_1 + \alpha_3 = \pi$ and $\delta = \frac{\pi}{5}$, and consequently there is no way to satisfy condition (1.1), or we get the configuration illustrated in Figure 8(b). According to the spherical triangle (18, 19, 20, 29), de-

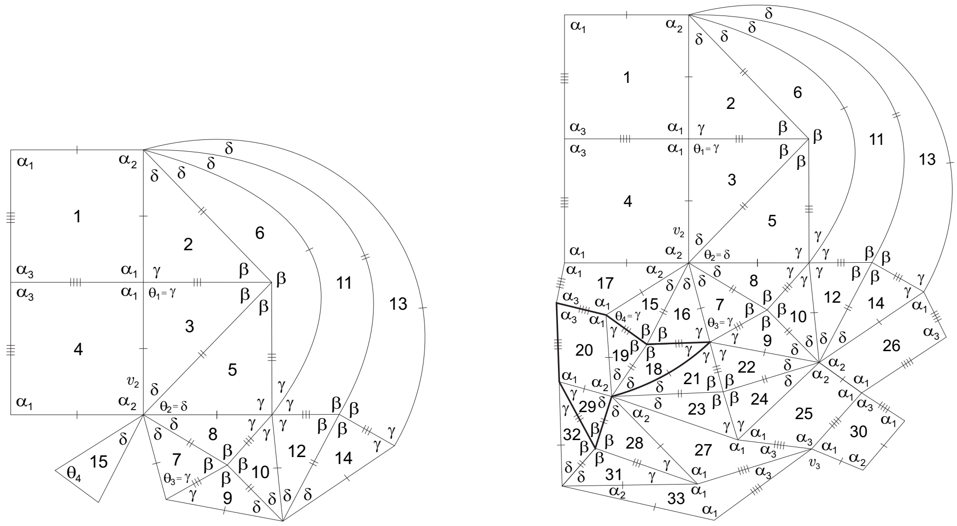

(a) (b)

Figure 8: Local configurations

limited by the dark line, we have $\alpha_3 + \gamma > \frac{\pi}{2}$, which implies $\alpha_3 > \frac{\pi}{6}$. Nevertheless, at vertex v_3 we reach an impossibility. On the other hand, if $\theta_4 = \beta$, we get the configuration illustrated in Figure 9. Note that we cannot have $\alpha_3 + \alpha_3 = \pi$, as $\alpha_2 > \alpha_3$ and $\delta > \frac{\pi}{6}$. At vertex v_3 we must have $k\alpha_3 = \pi$, with $k \geq 3$. Moreover, using (1.1), we obtain

$$4 \sin \frac{\delta}{2} \cos \frac{\pi}{2k} = 1,$$

and consequently $k < 6$. For each $k \in \{3, 4, 5\}$, we obtain a single tiling, denoted by $\mathcal{J}_k$. We have $\beta = \frac{\pi}{2}$, $\alpha_1 + \gamma = \pi$, $\alpha_2 + 3\delta = \pi$, $\gamma = \frac{\pi}{3}$, $k\alpha_3 = \pi$, and $\delta = 2 \arcsin \frac{1}{4 \cos \frac{\pi}{2k}}$. 3D representations of $\mathcal{J}_k$, $k = 3, 4, 5$, are given in Figure 10.

(iii)−2. Suppose now that $\theta_3 = \beta$. As in the previous case, we must have $t = 2$ or $t = 3$ (note that if $t \geq 3$, we must have $3\gamma = \pi$).

If $t = 2$, the last configuration is uniquely extended to the planar representation illustrated in Figu-re 11, where $k\alpha_3 = \pi$, $k \geq 2$. Using (1.1), we get

$$\delta = \delta_k(\gamma) = \arcsin \left(\frac{\cos \gamma}{\cos \frac{\pi}{2k}} \right),$$

where $0 < \delta < \gamma < \frac{\pi}{2}$ and $k \geq 2$. In Figure 12 is outlined the graphic of this function for $\frac{\pi}{2k} \leq \gamma < \frac{\pi}{2}$. We shall denote the family of f-tilings of Figure 11 by $\mathcal{S}^k_\gamma$, with $\beta = \frac{\pi}{2}$, $\alpha_1 + \gamma = \pi$, $\alpha_2 + 2\delta = \pi$, $k\alpha_3 = \pi$, with $k \geq 2$ and $\gamma \in \left(\gamma^k_{\min}, \gamma^k_{\max}\right]$. As $\delta <$

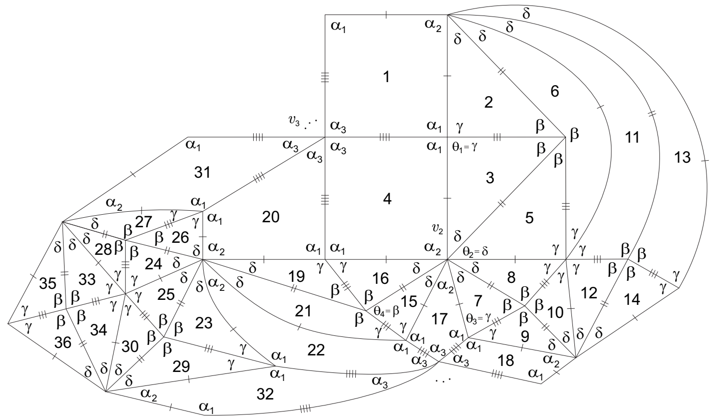

Figure 9: Planar representation of $\mathcal{J}_k$, $k = 3, 4, 5$

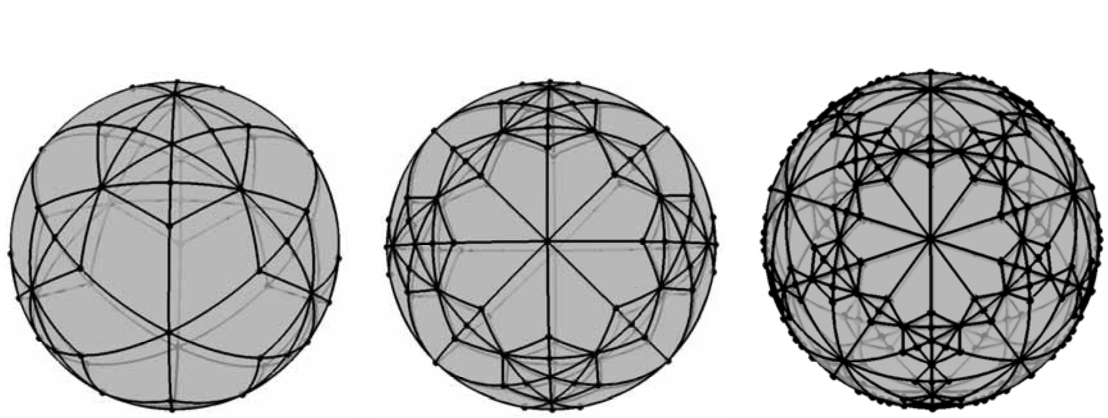

(a) (b) (c)

Figure 10: f-tilings $\mathcal{J}_k$, $k = 3, 4, 5$

$\gamma \leq 2\delta$, it is easy to obtain $\gamma^k_{\min} = \arctan \frac{1}{\cos \frac{\pi}{2k}}$ and $\gamma^k_{\max} = 2 \arcsin \frac{\sqrt{8+\cos^2 \frac{\pi}{2k}} - \cos \frac{\pi}{2k}}{4}$. 3D representations of $\mathcal{S}^2_\gamma$ and $\mathcal{S}^3_\gamma$ are given in Figure 13.

If $t = 3$, we obtain the configuration illustrated in Figure 14(a). Note that $\theta_4 = \delta$ implies the existence of angles α_2 and γ glued surrounding vertex v_2. Now, at vertex v_3, we have $\alpha_2 + \delta + \alpha_2 = \pi$ or $\alpha_2 + 3\delta = \pi$. The first case is not possible, as it implies $\delta = \frac{\pi}{5}$ and no solution exist for equation (1.1). In the second case, if $\alpha_3 + \alpha_3 = \pi$, we obtain a contradiction, as $\alpha_2 > \alpha_3$ and $\delta > \frac{\pi}{6}$; otherwise, if $\alpha_3 + \alpha_3 < \pi$, we must have $k\alpha_3 = \pi$, with $k \geq 3$, as illustrated in Figure 14(b). In fact, it is not possible to have an angle α_1 surrounding vertex v_4, as $\alpha_1 = \frac{2\pi}{3}$ and, according to the area of the spherical triangle (1, 2, 23, 24), we have $\alpha_3 > \frac{\pi}{6}$. The remaining analysis was already presented, since the last configuration is coincident with the one illustrated in Figure 9.

2. Suppose finally that $\alpha_1 + \gamma < \pi$. In this case, we have necessarily $\alpha_1 + \gamma + k\alpha_3 = \pi$, with $k \geq 1$, as illustrated in Figure 15. We reach a contradiction, since there is no

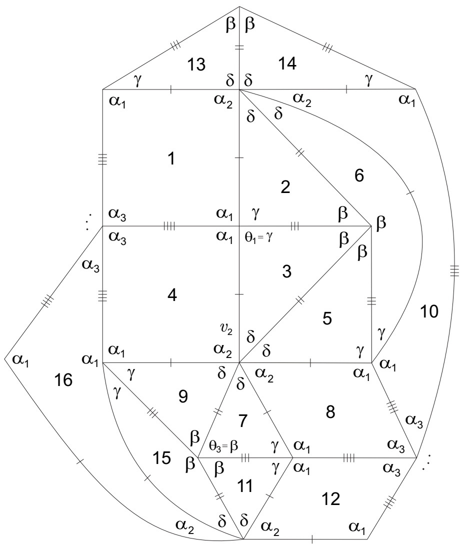

Figure 11: Planar representation of $\mathcal{S}_\gamma^k$, with $k \geq 2$ and $\gamma \in \left(\gamma_{\min}^k, \gamma_{\max}^k\right]$

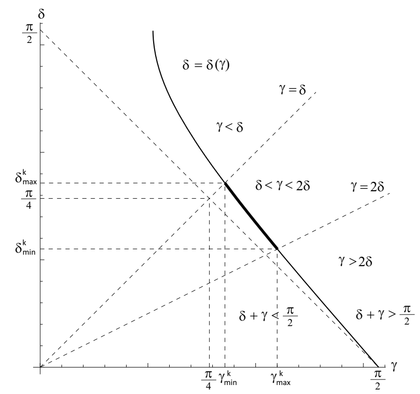

Figure 12: $\delta = \delta_k(\gamma) = \arcsin\left(\frac{\cos\gamma}{\cos\frac{\pi}{2k}}\right)$, $\frac{\pi}{2k} \leq \gamma < \frac{\pi}{2}$ and $k \geq 2$

way to satisfy the angle-folding relation around vertex v (note that $\theta_2 = \delta$ forces the existence of angles α_2 and γ glued). □

Proposition 2.2. *If $\alpha_2 > \alpha_1, \alpha_3$, then $\Omega(K,T) \neq \varnothing$ if and only if*

(i) $\alpha_1 + \gamma = \pi,\ \ \alpha_2 + \delta = \pi,\ \ \beta = \frac{\pi}{2}$ *and* $\alpha_1 + \alpha_3 = \pi$, *or*

(ii) $\alpha_1 + \gamma = \pi,\ \ \alpha_2 + 2\delta = \pi,\ \ \beta = \frac{\pi}{2}$ *and* $k\alpha_3 = \pi$, *with* $k \geq 2$, *or*

(iii) $\alpha_1 + 2\gamma = \pi,\ \ \alpha_2 + \delta = \pi,\ \ \beta = \frac{\pi}{2},\ \ \alpha_1 + \alpha_3 = \pi$ *and* $k\delta = \pi$, *with* $k \geq 4$.

In the first situation, $\Omega(K,T)$ is composed by a continuous family of f-tilings, denoted by $\mathcal{G}_\gamma$, with $\gamma \in \left(\frac{\pi}{4}, \frac{\pi}{2}\right)$.

In the second situation, the angles γ and δ satisfy $\cos\gamma = \cos\frac{\pi}{2k}\sin\delta$ and for each $k \geq 2$, $\Omega(K,T)$ is composed by a continuous family of f-tilings, say $\mathcal{S}_\gamma^k$, with

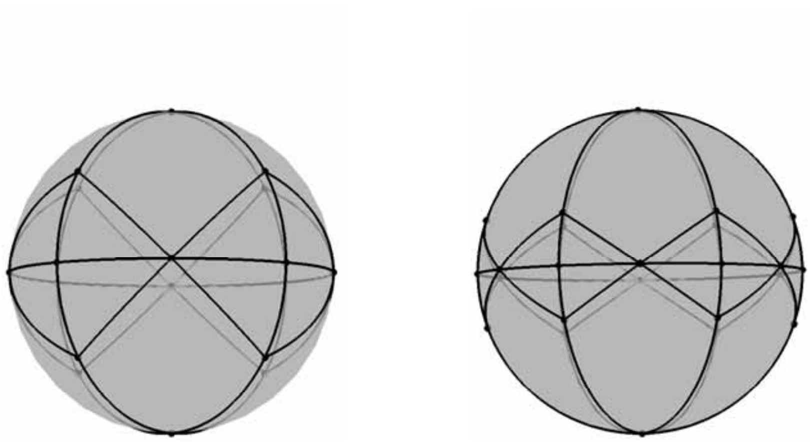

(a) $k = 2$ (b) $k = 3$

Figure 13: f-tiling $\mathcal{S}_\gamma^k$, with $\gamma \in \left(\gamma_{\min}^k, \gamma_{\max}^k\right]$

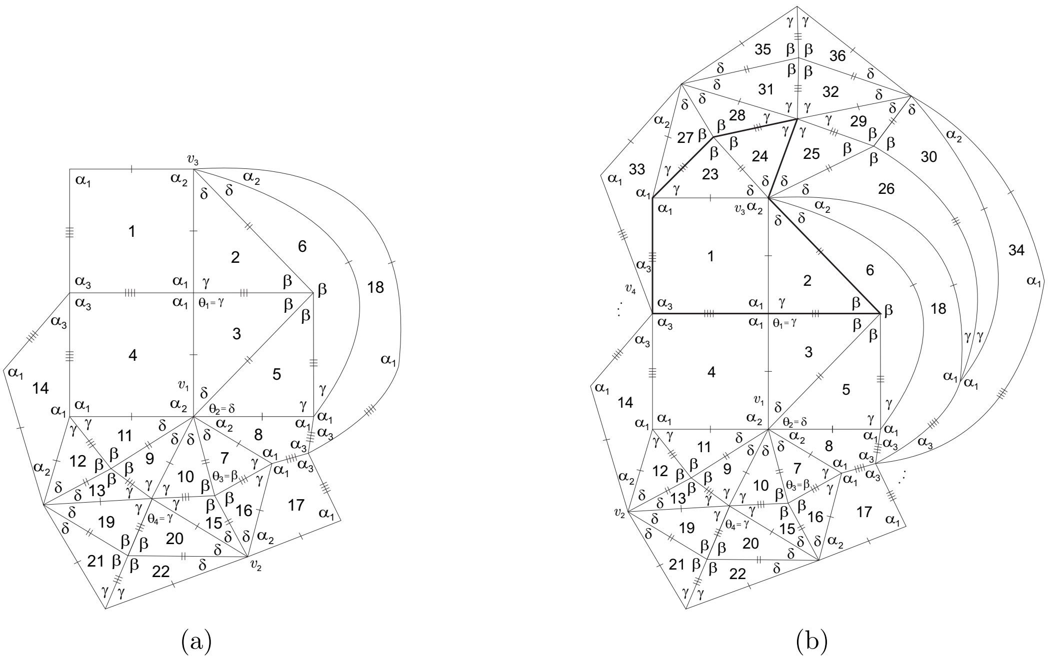

(a) (b)

Figure 14: Local configurations

$\gamma \in \left(\gamma_{\min}^k, \frac{\pi}{2}\right)$, where

$$\gamma_{\min}^k = 2 \arcsin \frac{\sqrt{8 + \cos^2 \frac{\pi}{2k}} - \cos \frac{\pi}{2k}}{4}.$$

In the last case, for each $k \geq 4$, $\Omega(K,T)$ is composed by a single f-tiling, denoted by $\mathcal{M}^k$.

Remark. Planar and 3D representations of $\mathcal{G}_\gamma$ are illustrated in Figure 16(b) and Figure 18, respectively. A planar representation of $\mathcal{S}_\gamma^k$ is illustrated in Figure 11. For

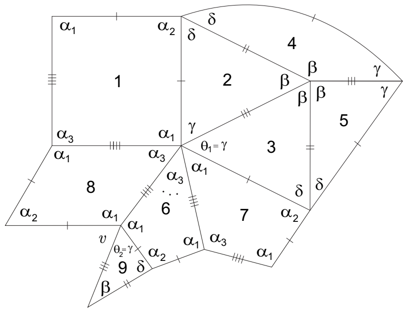

Figure 15: Local configurations

3D representations of $\mathcal{S}_\gamma^2$ and $\mathcal{S}_\gamma^3$ see Figure 20. The planar representation of $\mathcal{M}^k$ is illustrated in Figure 22(b). 3D representations of $\mathcal{M}^k$, for $k = 4$ and $k = 5$, are given in Figure 23.

Proof. Suppose that any f-tiling with K and T has at least two cells congruent, respectively, to K and T, such that they are in adjacent positions as illustrated in Figure 2-II and $\alpha_2 > \alpha_1, \alpha_3$ $\left(\alpha_2 > \frac{\pi}{2}\right)$.

As in the previous proposition, with the labeling of Figure 3(a), at vertex v_1 we have $\theta_1 = \gamma$ (it is a straightforward exercise to show that $\alpha_1 + \beta + \rho \leq \pi$, with $\rho \in \{\alpha_1, \alpha_3, \delta\}$, lead to a vertex surrounded by angles α_2 and γ glued or an incompatibility between sides at vertex v_1). Also, at vertex v_1 we have $\alpha_1 + \gamma = \pi$ or $\alpha_1 + \gamma < \pi$.

1. Suppose firstly that $\alpha_1 + \gamma = \pi$. The configuration of Figure 3(a) is uniquely extended to the one illustrated in Figure 16(a). At vertex v_2 we have

$$\alpha_2 + \delta = \pi \quad \text{or} \quad \alpha_2 + \delta < \pi.$$

1.1 If $\alpha_2 + \delta = \pi$, a complete planar representation is achieved; see Figure 16(b). Note that $\alpha_1 + \alpha_3 = \pi$, otherwise we reach a vertex surrounded by angles α_2 and γ glued, which is not possible.

As $0 < \delta < \gamma < \frac{\pi}{2}$, and using (1.1), we obtain

$$\cos\gamma - 2\sin\frac{\delta}{2}\cos\frac{\gamma}{2} = 0,$$

which means that

$$\delta = \delta(\gamma) = 2\arcsin\left(\frac{\cos\gamma}{2\cos\frac{\gamma}{2}}\right).$$

In Figure 17 is outlined the graphic of this function for $0 < \gamma < \frac{\pi}{2}$. We shall denote the family of f-tilings obtained from Figure 16(b) by $\mathcal{G}_\gamma$, with $\beta = \frac{\pi}{2}$, $\alpha_1 + \alpha_3 = \alpha_1 + \gamma = \pi$, $\alpha_2 + \delta = \pi$, and $\gamma \in \left(\frac{\pi}{4}, \frac{\pi}{2}\right)$. A 3D representation of $\mathcal{G}_\gamma$ is given in Figure 18.

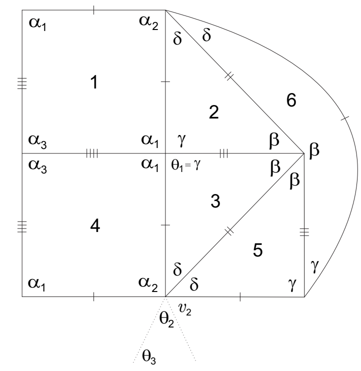

(a)

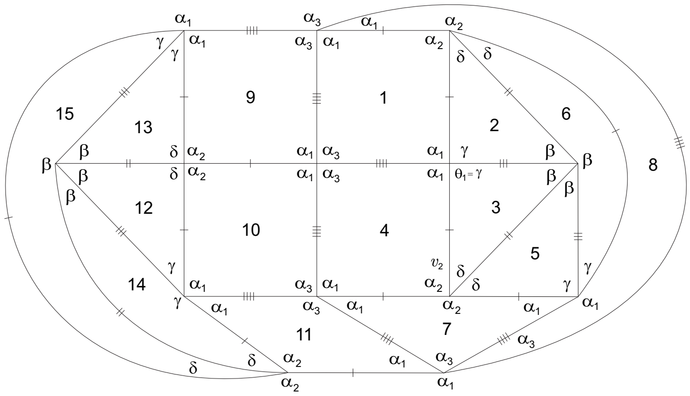

(b) Planar representation of $\mathcal{G}_\gamma$, $\gamma \in \left(\frac{\pi}{4}, \frac{\pi}{2}\right)$

Figure 16: Local configurations

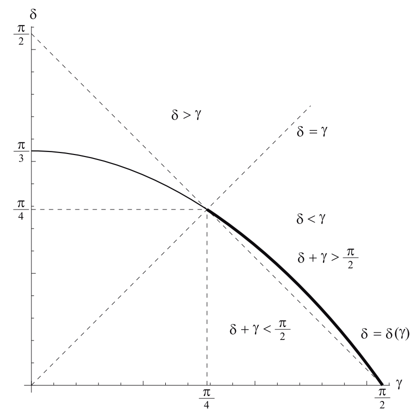

Figure 17: $\delta = \delta(\gamma) = 2 \arcsin\left(\frac{\cos\gamma}{2\cos\frac{\gamma}{2}}\right)$, $0 < \gamma < \frac{\pi}{2}$

1.2 Suppose now that $\alpha_2 + \delta < \pi$ (Figure 16(a)). In this case, we must have $\alpha_2 + t\delta = \pi$, with $t \geq 2$ (note that, if there exist at least one angle α_3 in this alternated sum, then the other sum must contain two angles α_1, but $\alpha_1 > \beta = \frac{\pi}{2}$), and so $\theta_2 = \delta$.

It is a straightforward exercise to show that if $t > 2$, we have necessarily a vertex surrounded by six angles γ. Nevertheless, as α_2 and $\gamma + \delta$ are greater than $\frac{\pi}{2}$, we

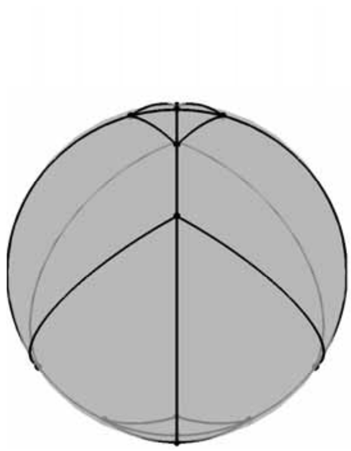

Figure 18: f-tilings $\mathcal{G}_\gamma$, with $\gamma \in \left(\frac{\pi}{4}, \frac{\pi}{2}\right)$

obtain $\alpha_2 + t\delta + 3\gamma > 2\pi$, which is not possible. Therefore, we must have $t = 2$ and we will distinguish the cases $\theta_3 = \gamma$ and $\theta_3 = \beta$.

1.2.1 If $t = 2$ and $\theta_3 = \gamma$, we get the configuration of Figure 6(b). As $\alpha_2 > \alpha_1$, we obtain an impossibility.

1.2.2 Consider that $t = 2$ and $\theta_3 = \beta$. The last configuration is uniquely extended to get the planar representation similar to the one illustrated in Figure 11, where

$$\alpha_1 + \gamma = \pi, \qquad \alpha_2 + 2\delta = \pi, \qquad \beta = \frac{\pi}{2} \qquad \text{and} \qquad k\alpha_3 = \pi, \;\; k \geq 2.$$

In Figure 19 is outlined the graphic of this function for $\frac{\pi}{2k} \leq \gamma < \frac{\pi}{2}$. Following the notation used in Proposition 2.1, we denote this family of f-tilings by $\mathcal{S}^k_\gamma$, with $\beta = \frac{\pi}{2}$, $\alpha_1 + \gamma = \pi$, $\alpha_2 + 2\delta = \pi$, $k\alpha_3 = \pi$, with $k \geq 2$ and $\gamma \in \left(\gamma^k_{\min}, \frac{\pi}{2}\right)$. As $\gamma > 2\delta$, it is easy to obtain $\gamma^k_{\min} = 2 \arcsin \frac{\sqrt{8+\cos^2 \frac{\pi}{2k}} - \cos \frac{\pi}{2k}}{4}$. 3D representations of $\mathcal{S}^2_\gamma$ and $\mathcal{S}^3_\gamma$ are given in Figure 20.

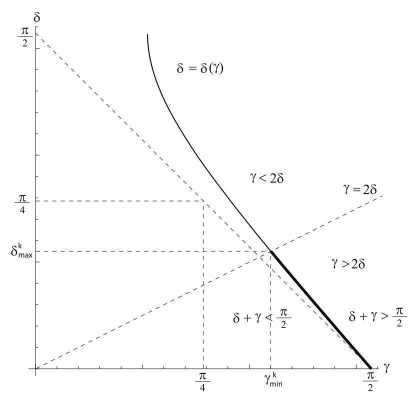

Figure 19: $\delta = \delta_k(\gamma) = \arcsin\left(\frac{\cos\gamma}{\cos\frac{\pi}{2k}}\right)$, $\frac{\pi}{2k} \leq \gamma < \frac{\pi}{2}$ and $k \geq 2$

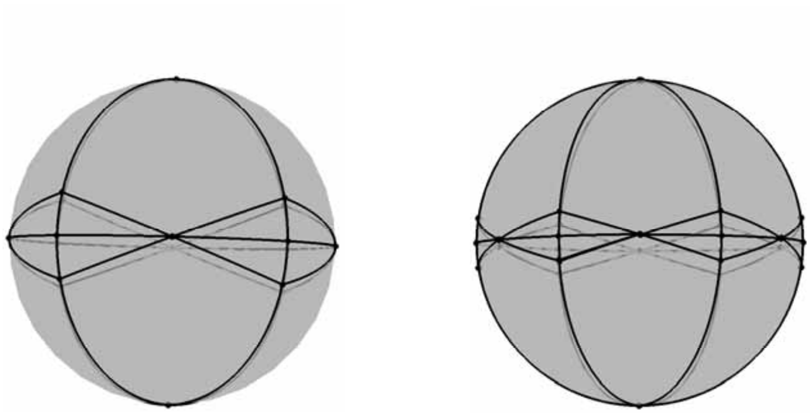

(a) $k = 2$ (b) $k = 3$

Figure 20: f-tiling $\mathcal{S}_{\gamma}^{k}$, with $\gamma \in \left(\gamma_{\min}^{k}, \frac{\pi}{2}\right)$

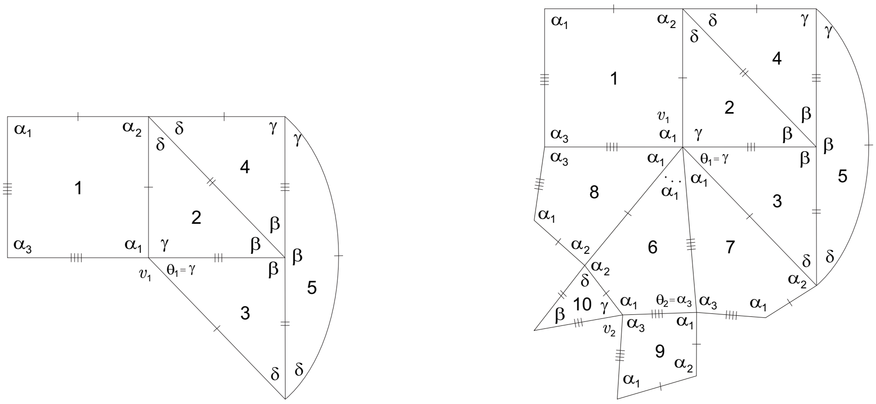

(a) (b)

Figure 21: Local configurations

2. Suppose now that $\alpha_1 + \gamma < \pi$, as illustrated in Figure 21(a). Using the fact that two cells congruent to K and T cannot be in adjacent positions as in the first case of adjacency, at vertex v_1 we can have only one of the following possibilities:

(i) $\alpha_1 + \gamma + k\alpha_1 = \pi$, $k \geq 1$;

(ii) $\alpha_1 + \gamma + \gamma = \pi$;

(iii) $\alpha_1 + \gamma + k\alpha_3 = \pi$, $k \geq 1$.

(i) Suppose that $\alpha_1 + \gamma + k\alpha_1 = \pi$, with $k \geq 1$, as illustrated in Figure 21(b). Consequently we have $\alpha_3 > \frac{\pi}{2}$ (note that $(\alpha_1 + \gamma + \alpha_1) + (\alpha_2 + \delta) + (\beta + \beta) \leq (\beta + \gamma + \delta) + (2\alpha_1 + \alpha_2 + \beta) \leq 3\pi$ and $(\beta + \gamma + \delta) + (2\alpha_1 + \alpha_2 + \alpha_3) > 3\pi$). Avoiding the existence of a triangle and a kite in adjacent positions as in the first case of adjacency, we remark that it is not possible to include angles δ in this alternated angle sum and also we must have $\theta_2 = \alpha_3$. Due to the edge lengths, vertex v_2

cannot have valency four. Nevertheless, as $\alpha_3 > \beta$, we have $\alpha_3 + \gamma + \rho > \pi$, for all $\rho \in \{\alpha_1, \alpha_2, \alpha_3, \beta, \gamma, \delta\}$.

(ii) If $\alpha_1 + \gamma + \gamma = \pi$, we must have $k\delta = \pi$, with $k \geq 4$ (Figure 22(a)). As

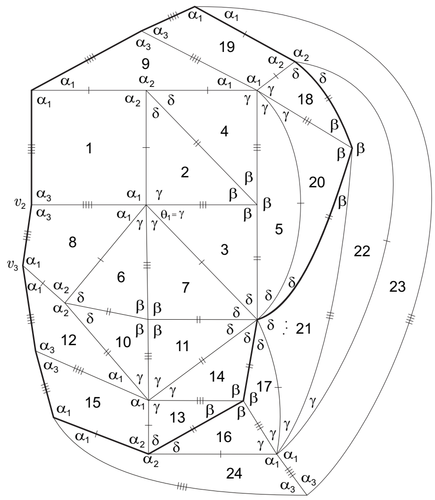

(a)

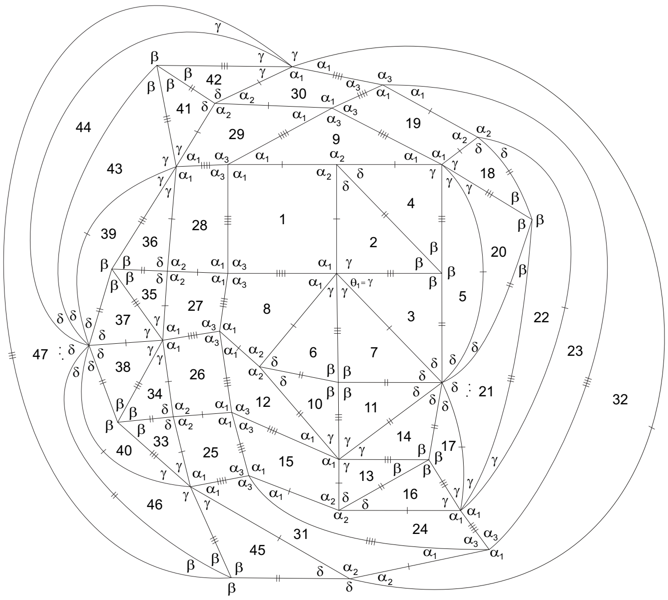

(b) Planar representation of $\mathcal{M}^k$, $k \geq 4$

Figure 22: Local configurations

$\alpha_1 + \alpha_3 + \delta > \pi$, at vertex v_2 we have $\alpha_3 + \alpha_1 = \pi$. Note that we cannot have $\alpha_3 + \alpha_3 \leq \pi$ at this vertex. In fact, if $\alpha_3 + \alpha_3 \leq \pi$ and

- $\alpha_1 > \alpha_3$, we have $\alpha_1 + \alpha_1 + \rho \geq \alpha_1 + \alpha_3 + \delta > \pi$, for all $\rho \in \{\alpha_1, \alpha_2, \alpha_3, \beta, \gamma, \delta\}$, and $\alpha_1 = \frac{\pi}{2}$ is an impossibility as $2\gamma > \gamma + \delta > \frac{\pi}{2}$;

- $\alpha_1 \leq \alpha_3$, we have $\alpha_3 + \alpha_3 + \rho \geq \alpha_1 + \alpha_3 + \delta > \pi$, for all ρ, and so $\alpha_3 = \frac{\pi}{2}$. Due to the edge lengths and also using the fact that $\alpha_1 + \gamma > \alpha_3$, $\alpha_1 < 2\gamma$ and

$2\alpha_1 > \alpha_3$, at vertex v_3 we must have $\alpha_1+\alpha_1+\alpha_1=\pi$ or $\alpha_1+\alpha_1+\gamma=\pi$. Both cases lead to $\alpha_1=\gamma=\frac{\pi}{3}$, and by (1.1), we obtain $\delta=\frac{\pi}{6}$ $(k=6)$. Nevertheless, observing the dark line in Figure 22(a), delimiting an spherical quadrangle, we obtain $3\alpha_1>\pi$, which is a contradiction.

Observe that we have $\alpha_2+\delta=\pi$, as $\alpha_2+\delta+\alpha_i>\pi$, for all $i=1,2,3$, as $\pi=\alpha_1+\alpha_3<\alpha_1+\alpha_2$ and $\alpha_2>\alpha_1$; we also have $\alpha_2+\delta+\rho>\pi$, for all $\rho\in\{\beta,\gamma\}$, since $\beta+\delta+\gamma>\pi$; finally, if $\alpha_2+\delta+\delta\leq\pi$, we would have $\alpha_1>2\delta$ and $2\delta+2\gamma<\alpha_1+2\gamma=\pi$, which is an impossibility as $\beta=\frac{\pi}{2}$ implies $\delta+\gamma>\frac{\pi}{2}$.

The last configuration is then extended uniquely to the planar representation illustrated in Figu-re 22(b). For each $k\geq 4$, we denote this f-tiling by $\mathcal{M}^k$. We have $\beta=\frac{\pi}{2}$, $\alpha_1+2\gamma=\pi$, $\alpha_1+\alpha_3=\pi$, $\alpha_2+\delta=\pi$ and $k\delta=\pi$, $k\geq 4$. Moreover, using (1.1), we get $\gamma_k=\arccos\left(\frac{1+\sqrt{5}}{2}\sin\frac{\pi}{2k}\right)$. 3D representations of $\mathcal{M}^k$, for $k=4$ and $k=5$, are given in Figure 23.

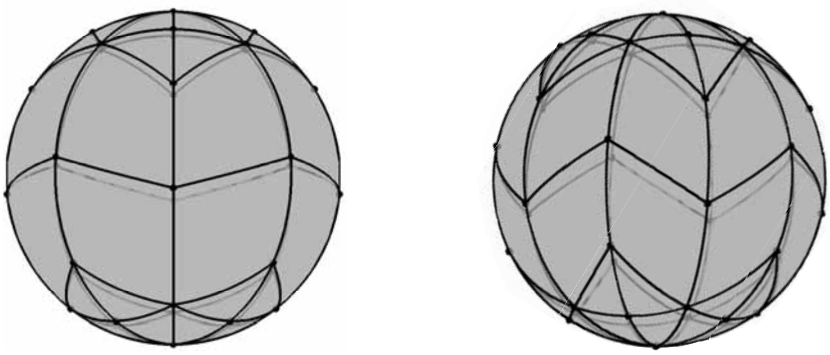

(a) $k=4$ (b) $k=5$

Figure 23: f-tiling $\mathcal{M}^k$, with $k\geq 4$

(iii) If $\alpha_1+\gamma+k\alpha_3=\pi$, $k\geq 1$, then $\delta>\alpha_3$ and consequently $\alpha_2+\alpha_3<\pi$. According to the area of the spherical kite K, we obtain $\alpha_1>\frac{\pi}{2}$. Nevertheless, observing Figure 24, an impossibility is reached at vertex v_2.

□

3 Combinatorial Structure

Let τ denote a spherical f-tiling. A spherical isometry σ is a symmetry of τ if σ maps every tile of τ into a tile of τ. The set of all symmetries of τ is a group under composition of maps, denoted by $G(\tau)$. Here, we classify the group of symmetries of the referred class of spherical f-tilings. Following the notation used in previous papers (e.g., [7]), and concerning the combinatorial structure of the f-tilings

- $\mathcal{M}^3$ (Figure 7), any symmetry of $\mathcal{M}^3$ fixes $N=(0,0,1)$ or maps N into $S=(0,0,-1)$. The symmetries that fix N are generated, for instance, by

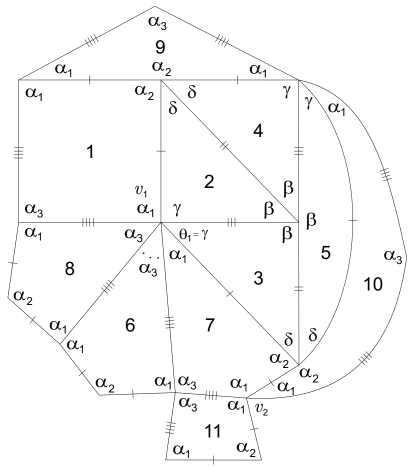

Figure 24: Local configuration

the rotation $R^z_{\frac{2\pi}{3}}$ and the reflection ρ^{yz}, giving rise to a subgroup G of $G(\mathcal{M}^3)$ isomorphic to D_3. To obtain the symmetries that send N into S it is enough to compose each element of G with $a = R^z_{\frac{\pi}{3}}\rho^{xy}$. We have

$$a^5\rho^{yz} = R^z_{\frac{5\pi}{3}}\rho^{xy}\rho^{yz} = R^z_{\frac{5\pi}{3}}R^y_{\pi} = R^y_{\pi}R^z_{\frac{\pi}{3}} = \rho^{yz}\rho^{xy}R^z_{\frac{\pi}{3}} = \rho^{yz}a,$$

$| < a > | = 6$ and $\rho^{yz} \notin < a >$. Therefore, $< a, \rho^{yz} >= G(\mathcal{M}^3) \simeq D_6$. $\mathcal{M}^3$ is 3-isohedral (three transitivity classes of tiles with respect to the group of symmetries) and 5-isogonal (five transitivity classes of vertices).

- $\mathcal{J}_k$, $k = 3, 4, 5$ (Figure 10), we have that
  - $\mathcal{J}_3$ has four vertices surrounded by six angles α_3, denoted by v_i, $i = 1, \ldots, 4$. Any symmetry of $\mathcal{J}_3$ that sends v_i into v_j, $i \neq j$, consists of a reflection on the great circle containing the remaining vertices. On the other hand, the symmetries of $\mathcal{J}_3$ fixing one of these four vertices form a subgroup G isomorphic to D_3. Thus, $G(\mathcal{J}_3)$ contains exactly 24 symmetries, and it is the group of all symmetries of the regular tetrahedron or the group of all permutations of four objects, S_4. Moreover, $\mathcal{J}_3$ is 4-tile-transitive and 7-vertex-transitive with respect to this group.
  - the symmetries of $\mathcal{J}_4$ that fix a vertex v of valency eight and surrounded by angles α_3 are generated by a reflection and by a rotation through an angle $\frac{\pi}{2}$ around the axis by $\pm v$. On the other hand, for any vertices v_1 and v_2 of this type, there is a symmetry of $\mathcal{J}_4$ sending v_1 into v_2. It follows that the symmetry group has exactly $48 = 6 \times 8$ elements and it forms the group of all symmetries of the cube $-$ the octahedral group $C_2 \times S_4$. $\mathcal{J}_4$ is 4-isohedral and 7-isogonal.
  - the group of symmetries that fix $(1, 0, 0)$ is precisely the 5th dihedral group D_5 generated by $R^x_{\frac{2\pi}{5}}$ and ρ^{xz}, for instance (similar situation occurs

to the remaining vertices of valency ten). On the other hand, there is always a symmetry of $\mathcal{J}_5$ that sends $(1,0,0)$ into any other vertex of the same type. This allows to conclude that $\mathrm{G}(\mathcal{J}_5)$ has exactly $12 \times 10 = 120$ elements. The ten kites surrounding vertex (1,0,0) (or other of the same type), along with the twenty adjacent triangles, form a dodecahedron and the symmetry group of $\mathcal{J}_5$ must be the icosahedral group $I_h = C_2 \times A_5$. Finally, it follows that $\mathcal{J}_5$ is 4-isohedral and 7-isogonal.

- $\mathcal{S}_\gamma^k$, $k \geq 2$ (Figure 13), any symmetry of $\mathcal{S}_\gamma^k$ fixes N or maps N into S. The symmetries that fix N are generated, for instance, by the rotation $R^z_{\frac{\pi}{k}}$ and the reflection ρ^{yz}, giving rise to a subgroup of $G(\mathcal{S}_\gamma^k)$ isomorphic to D_{2k}, the dihedral group of order $4k$. Now, the map $\phi = \rho^{xy}$ is a symmetry of $\mathcal{S}_\gamma^k$ that permutes N and S allowing us to get all the symmetries that map N into S. As ϕ commutes with $R^z_{\frac{\pi}{k}}$ and ρ^{yz}, it follows that $G(\mathcal{S}_\gamma^k)$ is isomorphic to $C_2 \times D_{2k}$. Moreover, $\mathcal{S}_\gamma^k$ has two transitivity classes of tiles, and so it is 2-isohedral. The vertices of $\mathcal{S}_\gamma^k$ form four transitivity classes.

- $\mathcal{G}_\gamma$, with $\gamma \in \left(\frac{\pi}{4}, \frac{\pi}{2}\right)$ (Figure 18), any symmetry of $\mathcal{G}_\gamma$ fixes N or maps N into S. The symmetries that fix N are generated, for instance, by the rotation R^z_π and the reflection ρ^{yz}, giving rise to a subgroup of $G(\mathcal{G}_\gamma)$ isomorphic to D_2. The map $\phi = R^z_{\frac{\pi}{2}} \circ \rho^{xy}$ is a symmetry of $\mathcal{G}_\gamma$ that permutes N and S. One has $\phi^3 \circ \rho^{yz} = \rho^{yz} \circ \phi$ and ϕ has order 4. It follows that ϕ and ρ^{yz} generate $G(\mathcal{G}_\gamma)$, and so it is isomorphic to D_4. $\mathcal{G}_\gamma$ is 2-tile-transitive and 4-vertex-transitive.

- $\mathcal{M}^k$, $k \geq 4$ (Figure 23), the group of symmetries that fix N is the kth dihedral group D_k generated by $R^z_{\frac{2\pi}{k}}$ and ρ^{yz}. The map $\phi = R^z_{\frac{\pi}{k}} \circ \rho^{xy}$ is a symmetry of $\mathcal{M}^k$ that permutes N and S, allowing us to get all the symmetries that map N into S. We have $\phi^{2k-1} \circ \rho^{yz} = \rho^{yz} \circ \phi$ and ϕ has order $2k$. It follows that ϕ and ρ^{yz} generate $G(\mathcal{M}^k)$, and so it is isomorphic to D_{2k}. $\mathcal{M}^k$ is 3-isohedral and 5-isogonal.

In Table 1 we summarize the combinatorial structure of all spherical dihedral f-tilings by kites and scalene triangles, with the shorter side of the kite equal to the longest side of the triangle within adjacency of type II. Our notation is as follows:

- $\delta_2 = \arcsin \frac{\sqrt{3}}{3}$; $\delta_k = 2 \arcsin \frac{1}{4 \cos \frac{\pi}{2k}}$, $k \in \{3,4,5\}$; $\delta_\gamma^k = \arcsin \left(\frac{\cos \gamma}{\cos \frac{\pi}{2k}} \right)$; $\gamma_{\min}^k = \arctan \frac{1}{\cos \frac{\pi}{2k}}$; $\delta_\gamma = 2 \arcsin \left(\frac{\cos \gamma}{2 \cos \frac{\gamma}{2}} \right)$; $\gamma_k = \arccos \left(\frac{1+\sqrt{5}}{2} \sin \frac{\pi}{2k} \right)$.

- M and N are, respectively, the number of triangles congruent to T and the number of kites congruent to K, used in the dihedral f-tilings.

- $G(\tau)$ is the symmetry group of each tiling $\tau \in \Omega\,(K,T)$; the indices of isohedrality and isogonality for the symmetry group are denoted, respectively, by #isoh. and #isog.

<table>
<tr><th colspan="2">f-tiling</th><th>$\boldsymbol{\alpha_1}$</th><th>$\boldsymbol{\alpha_2}$</th><th>$\boldsymbol{\alpha_3}$</th><th>$\boldsymbol{\beta}$</th><th>$\boldsymbol{\gamma}$</th><th>$\boldsymbol{\delta}$</th><th>M</th><th>N</th><th>$G(\tau)$</th><th>#isoh</th><th>#isog</th></tr>
<tr><td colspan="2">$\boldsymbol{\mathcal{M}^3}$</td><td>$\frac{2\pi}{3}$</td><td>$\pi - 2\delta_2$</td><td>$\frac{\pi}{3}$</td><td>$\frac{\pi}{2}$</td><td>$\frac{\pi}{3}$</td><td>$\delta_2$</td><td>24</td><td>12</td><td>D_6</td><td>3</td><td>5</td></tr>
<tr><td rowspan="3">$\boldsymbol{\mathcal{J}_k}$</td><td>$k = 3$</td><td rowspan="3">$\frac{2\pi}{3}$</td><td rowspan="3">$\pi - 3\delta_k$</td><td rowspan="3">$\frac{\pi}{k}$</td><td rowspan="3">$\frac{\pi}{2}$</td><td rowspan="3">$\frac{\pi}{3}$</td><td rowspan="3">$\delta_k$</td><td rowspan="3">$2^{5-k}3k!$</td><td rowspan="3">$2^{5-k}k!$</td><td>$S_4$</td><td>4</td><td>7</td></tr>
<tr><td>$k = 4$</td><td>$C_2 \times S_4$</td><td>4</td><td>7</td></tr>
<tr><td>$k = 5$</td><td>$C_2 \times A_5$</td><td>4</td><td>7</td></tr>
<tr><td colspan="2">$\boldsymbol{\mathcal{S}^k_\gamma}$, $\boldsymbol{k \geq 2}$</td><td>$\pi - \gamma$</td><td>$\pi - 2\delta^k_\gamma$</td><td>$\frac{\pi}{k}$</td><td>$\frac{\pi}{2}$</td><td>$\left(\gamma^k_{\min}, \frac{\pi}{2}\right)$</td><td>$\delta^k_\gamma$</td><td>$8k$</td><td>$4k$</td><td>$C_2 \times D_{2k}$</td><td>2</td><td>4</td></tr>
<tr><td colspan="2">$\boldsymbol{\mathcal{G}_\gamma}$</td><td>$\pi - \gamma$</td><td>$\pi - \delta_\gamma$</td><td>$\gamma$</td><td>$\frac{\pi}{2}$</td><td>$\left(\frac{\pi}{4}, \frac{\pi}{2}\right)$</td><td>$\delta_\gamma$</td><td>8</td><td>8</td><td>D_4</td><td>2</td><td>4</td></tr>
<tr><td colspan="2">$\boldsymbol{\mathcal{M}^k}$, $\boldsymbol{k \geq 4}$</td><td>$\pi - 2\gamma_k$</td><td>$\pi - \delta$</td><td>$2\gamma_k$</td><td>$\frac{\pi}{2}$</td><td>γ_k</td><td>$\frac{\pi}{k}$</td><td>$8k$</td><td>$4k$</td><td>D_{2k}</td><td>3</td><td>5</td></tr>
</table>

Table 1: Combinatorial Structure of the Dihedral f-tilings of S^2 by Kites and Scalene Triangles, with the shorter side of the kite equal to the longest side of the triangle and adjacency of type II

References

[1] C.P. Avelino and A.F. Santos, Spherical and planar folding tessellations by kites and equilateral triangles, *Australas. J. Combin.* **53** (2012), 109–125.

[2] C.P. Avelino and A.F. Santos, Spherical Folding Tesselations by Kites and Isosceles Triangles II, *Int. J. Pure Appl. Math.* **85(1)** (2013), 45–67.

[3] C.P. Avelino and A.F. Santos, Spherical Folding Tessellations by Kites and Isosceles Triangles: a Case of Adjacency, *Math. Commun.* **19** (2014), 1–28.

[4] C.P. Avelino and A.F. Santos, Spherical Folding Tessellations by Kites and Isosceles Triangles IV, *Ars Math. Contemp.* **11** (2016), 59–78.

[5] C.P. Avelino and A.F. Santos, Geometric and combinatorial structure of a class of spherical folding tesselations — I, *Czechoslovak Math. J.* (to appear).

[6] A.M. Breda, A class of tilings of S^2, *Geom. Dedicata* **44** (1992), 241–253.

[7] A.M. Breda and A.F. Santos, Symmetry Groups of a Class of Spherical Folding Tilings, i *Appl. Math. Inf. Sci.* **3(2)** (2009), 123–134.

[8] S.A. Robertson, Isometric folding of Riemannian manifolds, *Proc. Roy. Soc. Edinburgh Sect. A* **79** (1977), 275–284.

[9] Y. Ueno and Y. Agaoka, Classification of tilings of the 2-dimensional sphere by congruent triangles, *Hiroshima Math. J.* **32** (2002), 463–540.

(Received 24 Jan 2017; revised 3 June 2017, 8 July 2017)